

Prediction accuracy of surrogate models as chaos indicator for nonlinear beam dynamics

Yongjun Li,^{1,*} Jinyu Wan,^{2,3} Allen Liu,⁴ Yi Jiao,^{2,3} and Robert Rainer¹

¹*Brookhaven National Laboratory, Upton, New York 11973, USA*

²*Institute of High Energy Physics, Beijing 100049, China*

³*University of Chinese Academy of Sciences, Beijing 100049, China*

⁴*Department of Electrical and Computer Engineering,
Purdue University, West Lafayette, Indiana 47907, USA*

Surrogate models have been widely used in studying nonlinear dynamical systems, including modern particle accelerators. A different perspective of viewing beam dynamical system from the prediction discrepancy of surrogate models is presented. The prediction accuracy was observed worse when particle motion is more chaotic. Therefore, such property can be used as a chaos indicator in beam dynamical system optimization. This new method was demonstrated with the National Synchrotron Light Source II storage ring.

I. INTRODUCTION

Surrogate models have been widely used in studying nonlinear dynamical systems [1–5], including charged particle motion in modern accelerators [6–12]. These models are obtained by training either simulated data or experimental data, which have a high computational demand or require complicated experimental processing. If models can predict the dynamical system properties accurately with reduced resource requirements, they can be used for more efficient applications, such as system optimization. Given same amount of training data and the complexity of model structure, it was observed that the prediction accuracy became worse when the nonlinear motion was more chaotic. This indicates that the prediction accuracy of model itself is a metric of chaos for the system. Therefore, rather than training accurate models, their prediction accuracy can be used directly as the objective for nonlinear beam dynamics optimization. The advantage of this approach is that the requirement on the absolute accuracy of surrogate models is less demanding, and therefore can be structured with less complexity.

To further explain this approach, the remaining sections are outlined as follows: Sect. II introduces the correlation between the chaos of a beam dynamical system and the prediction accuracy of its surrogate models constructed with an artificial neural network (ANN) [13]. In Sect. III, the prediction accuracies of an one-turn transportation surrogate model are used as chaos indicators in optimizing a storage ring dynamic aperture. A brief summary is given in Sect. IV.

II. CHAOS AND MODEL PREDICTION ACCURACY

When studying the stability of charged particles in modern accelerators, implementation of particle tracking

is often necessary. To determine the dynamic aperture (DA) boundary, in which particle motion is stable would require such a simulation. During the design stage, a lot of time-consuming tracking simulations are needed to search for magnet lattices with sufficient DA. To boost the search process, surrogate models have been used to replace the original accelerator lattices. The accuracy of the models usually plays a crucial role in ensuring optimization converges in the desired direction. Modern accelerators are integrated with some strong nonlinear magnets. This can make reliable surrogate models difficult to construct. From another perspective, however, prediction accuracy of surrogate models can be a metric of chaos for particle motion.

Consider a storage ring accelerator composed of various magnetic elements, in which the transportation of a charged particle for single turn can be represented by a nonlinear transformation

$$\vec{X}_1 = M_{0 \rightarrow 1} \cdot \vec{X}_0$$

Where, \vec{X}_1 , \vec{X}_0 are the particle coordinates in the phase space, and $M_{0 \rightarrow 1}$ is the one-turn transportation map. Given the ring magnetic lattice, and using some simulated trajectories (\vec{X}_0, \vec{X}_1) as illustrated in Fig. 1, an ANN as illustrated in Fig. 2 can be trained as its surrogate model. For this investigation, discussed in greater detail in the next section, a simulated trajectory dataset was divided into a training set and a testing set. With the training set, an ANN model was constructed. The accuracy of the model was then measured by the mean squared error (MSE) between the testing set and its model prediction.

Using the National Synchrotron Light Source II (NSLS-II) storage ring [14] as an example, four special scenarios were studied to give readers an intuitive concept as illustrated in Fig. 3. First consider a special scenario in which the lattice doesn't include any nonlinear magnets. The one-turn map is a linear transportation. In this case the model can perfectly predict any testing trajectory to the level of computation numerical error as shown in the first row, because the system is a simple

* Email: yli@bnl.gov

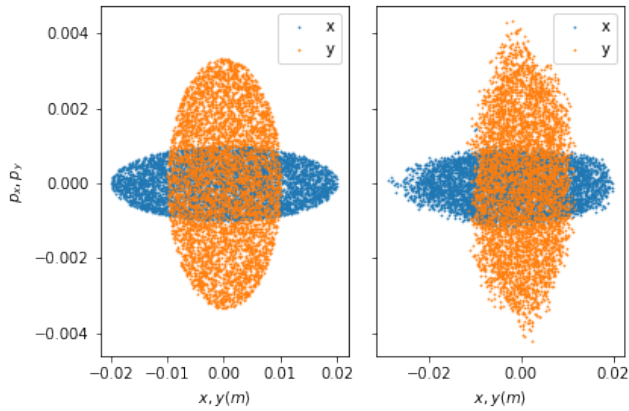


Figure 1. Simulated one-turn transportation of a storage ring lattice with a given input (left) and its output (right) in the 4-dimensional phase space.

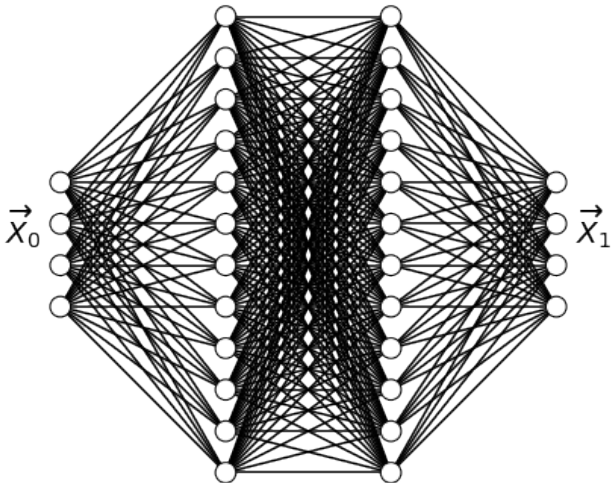


Figure 2. A four-layer $4 \times 12 \times 12 \times 4$ ANN used as the surrogate model to represent a storage ring's one-turn transportation in the 4-dimensional phase space.

linear transformation.

However, a linear lattice cannot maintain stable beam due to its intrinsic negative chromaticity [15]. The chromaticity represents a particle oscillation frequency shift due to its energy deviation. Therefore, some nonlinear sextupole magnets have to be integrated into the lattice to compensate for the inherent chromaticity. In the second scenario, the chromaticity was corrected to a value of positive 2 using chromatic sextupoles. After correction, the same structured ANN model saw significantly reduced prediction accuracy. This was due to nonlinear motion becoming chaotic, even unstable, when its trajec-

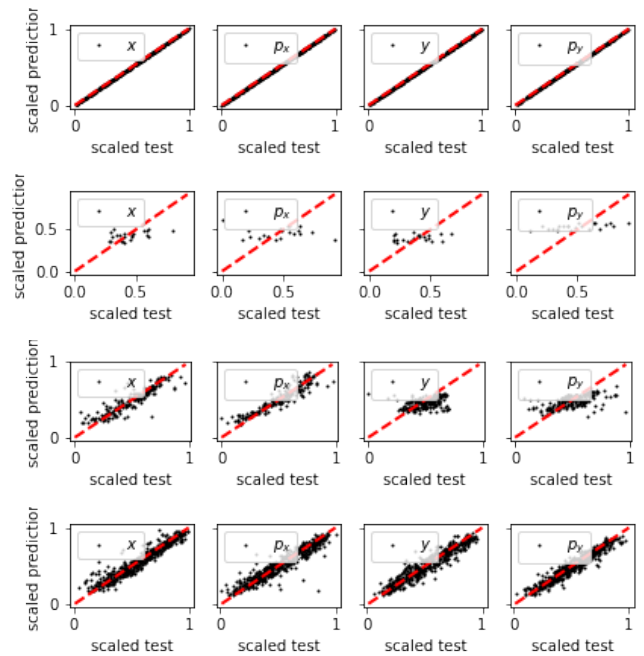


Figure 3. Prediction accuracies of the ANN model in four scenarios with different sextupole settings. Each subplot in a row represents one of the projected dimensions (x, p_x, y, p_y), in which each black dot represents one particle's scaled coordinate. The dashed red line represents the desired expectation. Row 1: a perfect surrogate for the purely linear lattice (black dots and the dashed red lines overlapped); Row 2: with only chromatic sextupoles in place, the prediction accuracies are poor; Row 3: improved accuracies were seen after some harmonic sextupoles are included, but their settings aren't optimal yet; Row 4: better accuracies were achieved after the harmonic sextupoles were well optimized.

tory diverged far from the origin. Due to strong nonlinearity, many particles fail to survive even for a single turn under this condition. As shown in row 2 of Fig. 3, low density clusters with large prediction discrepancies were observed there to represent the survived testing particles.

In the third scenario, extra harmonic sextupoles were included to compensate for the nonlinearity caused by the chromatic sextupoles. These sextupoles were not well optimized, so limited improvements on the accuracy were seen in row 3 of Fig. 3. The last scenario is that, after the harmonic sextupoles were well optimized, the chaos was dramatically mitigated, and most simulated particles survived for at least a single turn. Consequently, the accuracy of the ANN model is significantly improved as shown in row 4 of Fig. 3, in which high density clusters were distributed around the desired prediction line.

The correlations observed above indicate that the prediction accuracy of a surrogate model can be used as a chaos indicator. For a given structured ANN and similar amount of training data, the model prediction becomes more inaccurate when particle motion in a lattice is more chaotic. Therefore, rather than constructing complex, high performance models, the prediction accuracy them-

selves can be used as the objective for nonlinear lattice optimization.

III. APPLICATION

In this section, the prediction accuracy of an ANN model, used as a chaos indicator, was applied to optimize the nonlinear lattice of the NSLS-II ring. The NSLS-II [14] is a dedicated 3rd generation medium energy (3 GeV) light source operated by Brookhaven National Laboratory. Its main storage ring lattice is a traditional double-bend achromat structure. After the linear chromaticity is corrected by the chromatic sextupoles, the available “tuning knobs” used for DA optimization are six families of harmonic sextupoles.

A four-layer $4 \times 12 \times 12 \times 4$ ANN was chosen as the surrogate model to represent a one-turn transportation for on-momentum particles. The desired DA dimensions are $x = 25 \text{ mm}$ and $y = 10 \text{ mm}$ in the horizontal and vertical planes respectively at the injection point. Thus, two ellipses area in the phase space with the axes $(x, \frac{x}{\beta_x})$ and $(y, \frac{y}{\beta_y})$ are uniformly populated with 5,000 initial conditions, which is the input X_0 . Here $\beta_{x,y}$ are the local Twiss parameters [16]. The one-turn transportation can be accomplished with a symplectic particle tracking code, such as ELEGANT [17]. The coordinates at the exit are the output X_1 . 90% of the dataset is randomly chosen to train the ANN model using the python package KERAS [18], and the other 10% is used to test its prediction accuracy. The mean squared error (MSE) in each dimension is used as an independent optimization objective. By varying harmonic sextupole settings, the accuracy of the ANN model was monitored and used to drive a multi-objective genetic algorithm (MOGA) optimizer [19]. A good convergence of the average prediction accuracy was reached after 100th generation of evolution as shown in Fig. 4. Using 100 Intel[®] Xeon[®] 2.2-2.3 GHz CPU cores, optimization on this scale takes about 6 to 8 hours.

The DAs of the total population in the 100th generation were calculated. The histogram of their DA areas shows that most of candidates have a sufficient DA, with the smallest ones being greater than 400 mm^2 , which can well satisfy the requirement of machine operation.

To further confirm the correlation between the DA area and the ANN model’s accuracy, The DA areas and average prediction accuracy for all candidates in the 1st and 100th MOGA generations were computed for comparison. As shown in Fig. 6, the settings inside cluster A (the 1st generation) have relatively poor model prediction accuracy, and their DAs are small. Meanwhile, prediction accuracy in cluster B (the 100st generation) is significantly improved, as well as their DAs. Using this chaos indicator, which needs a very limited computation time, the nonlinear lattice optimization can be boosted significantly.

The candidate with the largest DA was chosen to im-

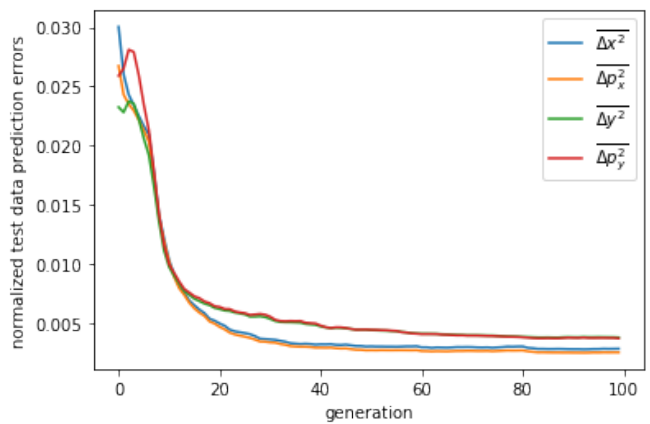


Figure 4. Convergence of prediction accuracy measured with four mean squared errors of test datasets in the MOGA optimization.

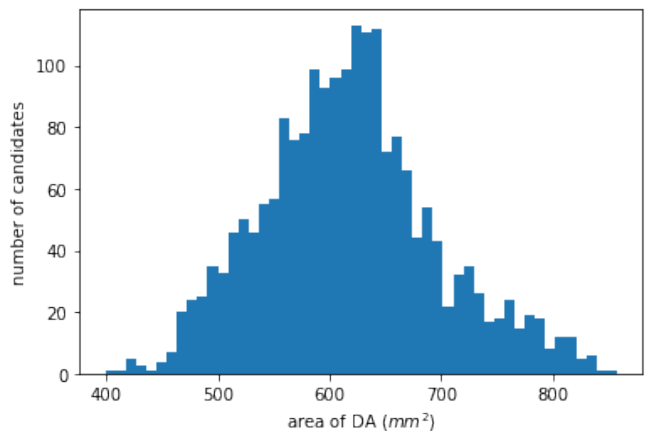


Figure 5. Distribution of the DA areas in the last generation of the MOGA optimization.

plement a detailed frequency map analysis (FMA) [20] and chaos map analysis [24] as shown in Fig. 7. Its DA is comparable to the solutions found using other methods [21–24]. In this case, not only was a fast DA optimization method provided (aided by machine-learning techniques), but a new perspective on nonlinear beam dynamics was observed with data science methods. This data-based chaos indicator is consistent with the existing rigorous nonlinear dynamics characterizations.

In this proof-of-principle study, only on-momentum particles in the 4-dimensional transverse phase space are used for demonstration purposes. They can be expanded to 5 or 6 dimensions to include the beam momentum or longitudinal motion as well.

In the example provided by the NSLS-II, a four-layer $4 \times 12 \times 12 \times 4$ ANN as shown in Fig. 2 was used. The selection of the numbers of hidden layers and nodes compromise between model accuracy and processing time. In principle, a more complicated ANN can achieve more accurate predictions but would need more data and time

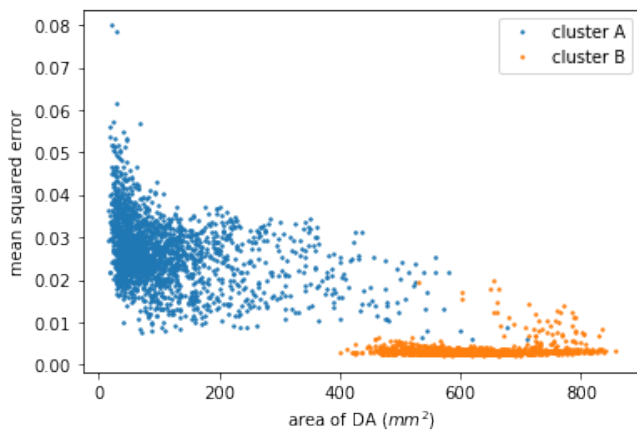


Figure 6. Correlation between the dynamic aperture and the ANN prediction accuracy seen in the MOGA optimization. The surrogate models of cluster A (Blue dots) have low accurate predictions due to greater chaotic motion, and therefore, their original lattices have smaller DAs. Meanwhile, prediction accuracies of cluster B are improved, as are their DAs.

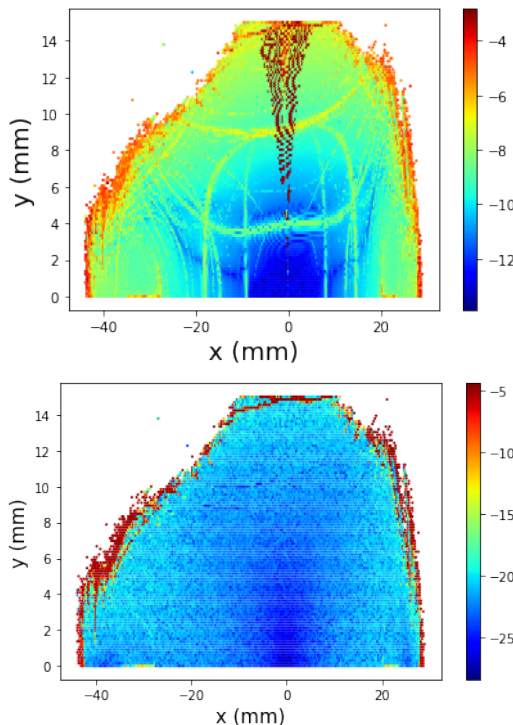


Figure 7. On-momentum particle frequency map analysis (top) and chaos map analysis (bottom) for the candidate with the largest DA. The color represents the tune diffusion rate [20] and the discrepancy between forward-reversal integrals [24] respectively due to the nonlinearity.

to train. For this application, high prediction accuracy is not critical because only relative accuracy is needed for the optimizer to converge. A three-layer ANN was also

tested and confirmed functional. However, its statistical fluctuations were larger than the one used here and therefore were not the focus of the investigation. Although, at the early stages of optimization, a simple structured, but computationally efficient ANN can be used to quickly narrow down the ranges of searching parameters. Then another, more complex ANN model can be deployed for a more accurate and precise search. Besides ANN, another surrogate model, multivariate polynomial response surfaces [25] was also confirmed to be able to see the existence of correlation. We believe some other surrogate models, such as support vector regression [26], etc. should be functional as well with this technique.

There are some other advanced machine-learning techniques available that can better evaluate accuracy of an ANN model. For example, using the K-fold cross validation method [27] ensures that every observation from the original dataset has the chance of appearing in training and test sets, especially when limited input data is available. In our example, rather than using the time-consuming cross-validation that K-fold offers, sufficient training data were generated with particle tracking simulation code, because using only one-turn tracking for the NSLS-II ring requires much less of a demand on computation resources.

IV. SUMMARY

A new data-based chaos indicator was introduced by correlating the nonlinearity of a dynamical system and its ANN surrogate model's prediction accuracy. This indicator can be directly used to optimize the dynamic aperture of storage rings. Traditionally, the prediction accuracy of a model has been critically important for many machine-learning applications. However, in this method, the prediction accuracy is used as a relative indicator of the chaos of a dynamical system. Greater accuracy is therefore less important, and surrogate models which have a lower resource demand, are sufficient for this purpose. Most importantly it provides a new perspective view on the severity of chaos in a nonlinear dynamical system.

ACKNOWLEDGMENTS

We would like to thank all NSLS-II accelerator physicists for the stimulating and collaborative discussions. This research is supported by the U.S. Department of Energy under Contract No. DE-SC0012704 (BNL), National Natural Science Foundation of China (No. 11922512) and Youth Innovation Promotion Association of Chinese Academy of Sciences (No. Y201904). A. Liu is supported by Virginia Pond Scholarship Summer Intern Program at BNL (2019).

-
- [1] Mauricio Barahona and Chi-Sang Poon, “Detection of nonlinear dynamics in short, noisy time series,” *Nature* **381**, 215–217 (1996).
- [2] Thomas Schreiber and Andreas Schmitz, “Improved surrogate data for nonlinearity tests,” *Phys. Rev. Lett.* **77**, 635–638 (1996).
- [3] Isao Tokuda, Takaya Miyano, and Kazuyuki Aihara, “Surrogate analysis for detecting nonlinear dynamics in normal vowels,” *The Journal of the Acoustical Society of America* **110**, 3207–3217 (2001).
- [4] Anand P Deshmukh and James T Allison, “Design of nonlinear dynamic systems using surrogate models of derivative functions,” in *ASME 2013 International Design Engineering Technical Conferences and Computers and Information in Engineering Conference* (American Society of Mechanical Engineers Digital Collection, 2013).
- [5] K Lindhorst, MC Haupt, and P Horst, “Efficient surrogate modelling of nonlinear aerodynamics in aerostructural coupling schemes,” *AIAA Journal* **52**, 1952–1966 (2014).
- [6] A Sanchez-Gonzalez, P Micaelli, C Olivier, TR Barillot, M Ilchen, AA Lutman, A Marinelli, T Maxwell, A Achner, M Agåker, *et al.*, “Accurate prediction of x-ray pulse properties from a free-electron laser using machine learning,” *Nature communications* **8**, 1–9 (2017).
- [7] Faya Wang, Minghao Song, Auralee Edelen, and Xiaobiao Huang, “Machine learning for design optimization of storage ring nonlinear dynamics,” arXiv preprint arXiv:1910.14220 (2019).
- [8] Xiaobiao Huang, Minghao Song, and Zhe Zhang, “Multi-objective multi-generation gaussian process optimizer for design optimization,” arXiv preprint arXiv:1907.00250 (2019).
- [9] Auralee Edelen, Nicole Neveu, Matthias Frey, Yannick Huber, Christopher Mayes, and Andreas Adelman, “Machine learning for orders of magnitude speedup in multiobjective optimization of particle accelerator systems,” *Phys. Rev. Accel. Beams* **23**, 044601 (2020).
- [10] Jinyu Wan, Paul Chu, and Yi Jiao, “Neural network-based multiobjective optimization algorithm for nonlinear beam dynamics,” *Phys. Rev. Accel. Beams* **23**, 081601 (2020).
- [11] M. Kranjčević, B. Riemann, A. Adelman, and A. Streun, “Multiobjective optimization of the dynamic aperture using surrogate models based on artificial neural networks,” *Phys. Rev. Accel. Beams* **24**, 014601 (2021).
- [12] Jun Zhu, Ye Chen, Frank Brinker, Winfried Decking, Sergey Tomin, and Holger Schlarb, “Deep learning-based autoencoder for data-driven modeling of an rf photoinjector,” arXiv preprint arXiv:2101.10437 (2021).
- [13] Mohamad H Hassoun *et al.*, *Fundamentals of artificial neural networks* (MIT press, 1995).
- [14] BNL, <https://www.bnl.gov/nsls2/project/PDR/>.
- [15] Shyh-Yuan Lee, *Accelerator physics* (World scientific publishing, 2018).
- [16] Ernest D Courant and Hartland S Snyder, “Theory of the alternating-gradient synchrotron,” *Annals of physics* **3**, 1–48 (1958).
- [17] Michael Borland, *Elegant: A flexible SDDS-compliant code for accelerator simulation*, Tech. Rep. (Argonne National Lab., IL (US), 2000).
- [18] Aurélien Géron, *Hands-on machine learning with Scikit-Learn, Keras, and TensorFlow: Concepts, tools, and techniques to build intelligent systems* (O’Reilly Media, 2019).
- [19] Kalyanmoy Deb, Amrit Pratap, Sameer Agarwal, and TAMT Meyarivan, “A fast and elitist multiobjective genetic algorithm: Nsga-ii,” *IEEE transactions on evolutionary computation* **6**, 182–197 (2002).
- [20] Jacques Laskar, “Introduction to frequency map analysis,” in *Hamiltonian systems with three or more degrees of freedom* (Springer, 1999) pp. 134–150.
- [21] Lingyun Yang, Yongjun Li, Weiming Guo, and Samuel Krinsky, “Multiobjective optimization of dynamic aperture,” *Physical Review Special Topics-Accelerators and Beams* **14**, 054001 (2011).
- [22] Yongjun Li and Lingyun Yang, “Multi-objective dynamic aperture optimization for storage rings,” *International Journal of Modern Physics A* **31**, 1644019 (2016).
- [23] Yongjun Li, Weixing Cheng, Li Hua Yu, and Robert Rainer, “Genetic algorithm enhanced by machine learning in dynamic aperture optimization,” *Physical Review Accelerators and Beams* **21**, 054601 (2018).
- [24] Yongjun Li, Yue Hao, Kilean Hwang, Robert Rainer, An He, and Ao Liu, “Fast dynamic aperture optimization with forward-reversal integration,” *Nuclear Instruments and Methods in Physics Research Section A: Accelerators, Spectrometers, Detectors and Associated Equipment* **988**, 164936 (2021).
- [25] George EP Box, J Stuart Hunter, *et al.*, “Multi-factor experimental designs for exploring response surfaces,” *The Annals of Mathematical Statistics* **28**, 195–241 (1957).
- [26] Alex J Smola and Bernhard Schölkopf, “A tutorial on support vector regression,” *Statistics and computing* **14**, 199–222 (2004).
- [27] Yoshua Bengio and Yves Grandvalet, “No unbiased estimator of the variance of k-fold cross-validation,” *Journal of machine learning research* **5**, 1089–1105 (2004).